THE JOURNAL OF PHYSICAL CHEMISTRY Letters

Letter

pubs.acs.org/JPCL

The Mechanochemistry of a Structural Zinc Finger

Judit Perales-Calvo, Ainhoa Lezamiz, and Sergi Garcia-Manyes*

Department of Physics and Randall Division of Cell and Molecular Biophysics, King's College London, Strand, WC2R 2LS, London, United Kingdom

Supporting Information

ABSTRACT: Zinc fingers are highly ubiquitous structural motifs that provide stability to proteins, thus contributing to their correct folding. Despite the high thermodynamic stability of the $ZnCys_4$ centers, their kinetic properties display remarkable lability. Here, we use a combination of protein engineering with single molecule force spectroscopy atomic force microscopy (AFM) to uncover the surprising mechanical lability (~90 pN) of the individual Zn−S bonds that form the two equivalent zinc finger motifs embedded in the structure of the multidomain DnaJ chaperone. Rational mutations within the zinc coordinating residues enable direct identification of the chemical determinants that regulate the interplay between zinc binding—requiring the presence of all four cysteines—and disulfide bond formation. Finally, our observations show that binding to hydrophobic short peptides drastically increases the mechanical stability of DnaJ. Altogether, our experimental approach offers a detailed, atomistic vista on the fine chemical mechanisms that govern the nanomechanics of individual, naturally occurring zinc finger.

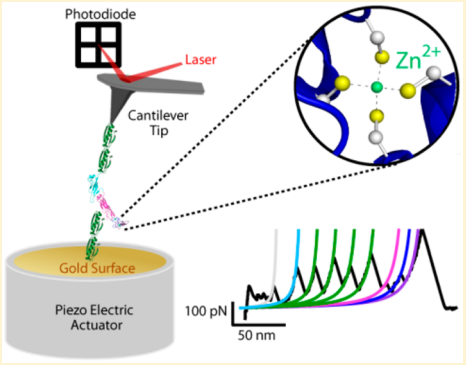

Metals are essential cofactors in around 50% of all proteins.[1,2] Zinc is the second most abundant transition metal in living organisms, carrying crucial functions for life.[3] The unique chemical properties of zinc finely regulate the nature of its coordination within the protein scaffold. In structural sites Zn^{2+} is tetrahedrally coordinated, mostly forming zinc finger conformations formed by ≥2 cysteines and ≤2 histidines. Structural zinc fingers are involved in the correct folding of proteins by stabilizing their tertiary structure.[4,5] Disruption of the individual zinc ligand bonds can lead to protein unfolding and to a loss in protein activity.[6] Hence, understanding the mechanisms by which zinc fingers rupture and reform provides new information on the folding mechanisms of metalloproteins, with important biological implications.[7]

The large biological significance of zinc contrasts with the limited amount of available biochemical techniques able to characterize the metal coordination sphere in biological zinc complexes,[6] especially due to the diamagnetic character of zinc and its lack of redox properties. Single molecule spectroscopy atomic force microscopy (AFM) has emerged as a powerful experimental tool to investigate the mechanical activation of individual chemical bonds.[8] The low forces required to unfold proteins (~10−200 pN), usually occurring through the disruption of a key patch of hydrogen bonds,[9] contrasts with the significantly higher (~0.5−2 nN) forces required to break homolytic and heterolytic covalent bonds,[10] and to activate chemical reactions.[11] More recently, this approach has been extended to the investigation of metalloproteins, mostly iron-based,[12−14] and also to study the effects of ligand[15] and metal binding[16] on the protein's mechanical resistance.[17]

In this Letter, we use single molecule force spectroscopy in combination with molecular biology engineering techniques to investigate the mechanical unfolding pathways of the structurally complex DnaJ Hsp40 chaperone, containing two consecutive highly conserved zinc fingers.[18,19] DnaJ, working alone or in combination with the Hsp70 (DnaK) chaperone family,[20] is involved in a wide variety of cellular functions, encompassing protein folding and transport, proteolysis, activation of transcription factors, and control of the redox state of different proteins.[18,19] Hence, guaranteeing the correct active, folded form of the protein is of capital importance for the cell. Our experiments provide new insights into the mechanochemistry of individual Zn−S bonds,[21] which is finely regulated by the chemical composition of the zinc finger motif.

An active truncated $DnaJ_{\Delta 107}$ (Figure 1A) protein containing three distinct domains (Domain I, II and III) was bracketed between two Protein L modules at each side (Figure 1B) and stretched in our AFM setup at a constant velocity of 400 nm s^{-1}. The resulting unfolding trajectories displayed a sawtooth pattern with unfolding peaks of alternating mechanical stability (Figure 1C). Such scenario is evocative of an unfolding mechanism whereby a mechanically labile domain remains protected from the effect of force until a more resilient domain unfolds first.[22,23] The four unfolding peaks eliciting $\Delta L_c \sim 19$ nm as revealed by WLC fits (Figure 1D) occurring at forces of ~140 pN (Figure 1E) correspond to the unfolding of the well-characterized PL marker (green fits).[24,25] The remaining four

Received: June 26, 2015
Accepted: August 3, 2015
Published: August 3, 2015

DOI: 10.1021/acs.jpclett.5b01371
J. Phys. Chem. Lett. 2015, 6, 3335−3340

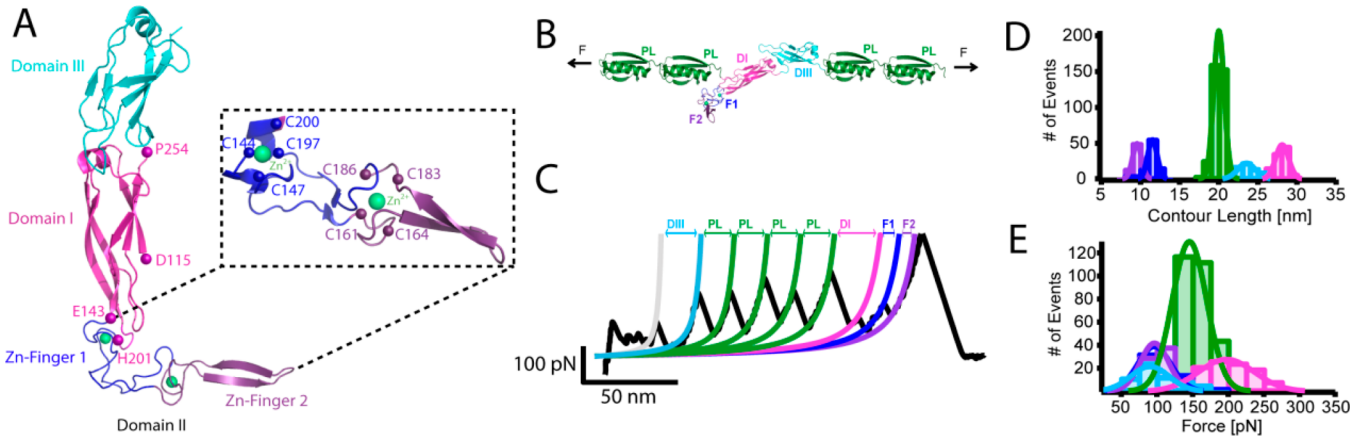

Figure 1. Sequential mechanical unfolding of DnaJ does not follow a hierarchy in the mechanical stability. (A) The $DnaJ_{\Delta 107}$ mutant is composed of three distinct domains: (i) Domain I (pink); (ii) Domain II or Zn-Binding Domain, which contains two zinc finger motifs (blue and purple; PDB: 1exk[18]); and (iii) Domain III (cyan). (B) Scheme of the engineered $(PL)_2DnaJ_{\Delta 107}(PL)_2$ polyprotein. (C) Typical force−extension trajectory corresponding to the mechanical unfolding of the $(PL)_2DnaJ_{\Delta 107}(PL)_2$ polyprotein. (D,E) Histograms corresponding to the contour length increase (D) and force (E) hallmarking each individual unfolding event.

unfolding peaks stem from the mechanical unfolding of $DnaJ_{\Delta 107}$. The first unfolding event characterized by ∼85 pN and $\Delta L_c \sim 23$ nm (cyan fit) is compatible with the unfolding of Domain III (Figure 1A, cyan and Table S1). A second high-force unfolding peak occurring at ∼187 pN with an associated $\Delta L_c \sim 28$ nm (pink fit) is likely to correspond to the unfolding of Domain I (Figure 1A). Domain II is composed of two consecutive zinc finger motifs that protrude out from Domain I (Figure 1A). The second zinc finger (Zf_2, purple) is inserted into the first finger (Zf_1, dark blue). Each finger motif contains four cysteines that coordinate an individual Zn^{2+} ion (green). Disrupting the first ZnS_4 center elicits $\Delta L_c \sim 11$ nm (blue fit, Figure 1C), whereas the mechanical disruption of the Zf_2 is hallmarked by $\Delta L_c \sim 9$ nm (purple fit, Figure 1C and Figure SI1). Surprisingly, the forces associated with these events are as low as ∼90 pN. This result is further confirmed by the low mechanical stability of each individual Zn-thiolate bond measured in the $(Zf_1Zf_2\text{-}I27)_4$ polyprotein (Figure SI2).

Thermal denaturation measured with bulk techniques showed that DnaJ unfolds via one or two intermediates;[26] these measurements, however, evaded structural characterization due to their ensemble-average nature. Follow-up CD experiments revealed that $DnaJ_{\Delta 107}$ exhibits a rather cooperative unfolding mechanism.[27] These experiments further demonstrated that releasing of Zn^{2+} from DnaJ decreased the overall stability of the entire protein.[26] An alternative hypothesis to explain the thermodynamic stabilization of the DnaJ structure in the Apo-protein was the putative presence of disulfide bonds between neighboring cysteines after Zn^{2+} release. However, direct observation and location of these disulfide bonds remained elusive.[26] In sharp contrast with these biochemistry experiments, our single molecule experiments reveal that when force is used as a denaturing agent, $DnaJ_{\Delta 107}$ unfolds following a well-defined, sequential pathway where each protein domain unfolds independently and does not follow a typical mechanical hierarchy scenario; once Domain III has unfolded, the mechanical disruption of both zinc finger motifs requires prior unfolding of the mechanically resilient Domain I, which acts as a mechanical protector[22] as further confirmed with analogous force-clamp experiments (Figure SI3). Crucially, zinc depletion only affects the mechanical stability of the zinc finger motifs, and does not affect the mechanical stability of the remainder protein (namely Domains I and III), thus confirming that zinc release is a highly localized event.

The measured forces required to disrupt the zinc fingers (∼90 pN) are surprisingly low, especially given the seemingly large Zn−S binding energies, of up to 185 kJ mol^{-1}.[28] Compared to the forces required to break a covalent bond, ranging from 0.8 to 2 nN,[10] the mechanical resistance of individual organometallic bonds has been found to be, in general, remarkably low, despite their relatively large covalent character. In particular, the mechanical forces required to break a Fe−S bond in rubredoxin are significantly lower than expected (∼210 pN).[12,21] The relative decrease in mechanical stability for the Zn−S bond compared to the Fe−S bond may be rationalized in terms of the higher ionic character of the Zn−S bond (and hence, of its smaller degree of covalency). Indeed, in the ZnS_4 complex, all the *d* orbitals of the metal are occupied, including the Zn $dx^2\text{-}y^2\text{-}S_{thiolate}$ $p\pi$, which cancels the π contribution to covalency.[29] In this vein, recent computational analysis suggest that the most commonly used description of the $[Zn(SR)_4]^{2-}$ center, involving a Lewis structure with four covalent σ S−Zn bonds, does not provide an accurate representation of the electronic environment around the zinc. Instead, a better representation of the electronic density is provided by four equivalent resonance structures whereby the central Zn cation forms one covalent and three ionic bonds to its four cysteine ligands. Such description is able to explain the generally high kinetic lability encountered in ZnS_4 cores despite the high Zn−S dissociation energy.[28] However, the measured forces for the Zn−S bond in DnaJ are still significantly lower than those observed for the Zn−S rupture found in modified rubredoxin (∼170 pN)[21] despite the almost identical bond lengths of the Zn−S center in each case (2.30 Å in DnaJ, PDB 1exk; 2.31 Å in rubredoxin, PDB 1zrp). These findings suggest that the protein environment, probably including the role of adjacent hydrogen bonds,[13,30] plays a crucial role in modulating the mechanical stability of the zinc finger.

To further investigate the role of the physicochemical properties of the zinc center on its nanomechanics, we first constructed a $DnaJ_{\Delta 107}$ Apo mutant ($DnaJ_{\Delta 107(C161/164/197/200S)}$) in which the two cysteines forming one of the two chelating motifs in each zinc finger were mutated to serines[31] to impair

DOI: 10.1021/acs.jpclett.5b01371
J. Phys. Chem. Lett. 2015, 6, 3335−3340

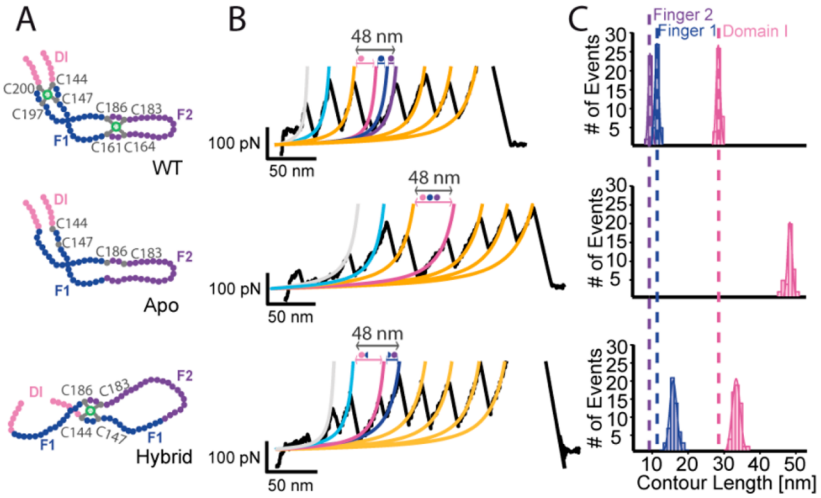

Figure 2. Both zinc finger motifs in DnaJ are able to hybridize in a non-native conformation. (A) Schematic representation of the residues that form the Zn-Binding Domain in $DnaJ_{\Delta 107}$ (top), $DnaJ_{\Delta 107(C161/164/197/200S)}$ in its Apo-form (middle) and $DnaJ_{\Delta 107(C161/164/197/200S)}$ in its hybrid form (bottom), and (B) their corresponding force−extension trajectories. (C) Histograms corresponding to the ΔL_c values associated with the unfolding of Domain I (pink) and the rupture of the first and second ZnS_4 centers (blue and purple) observed in each case.

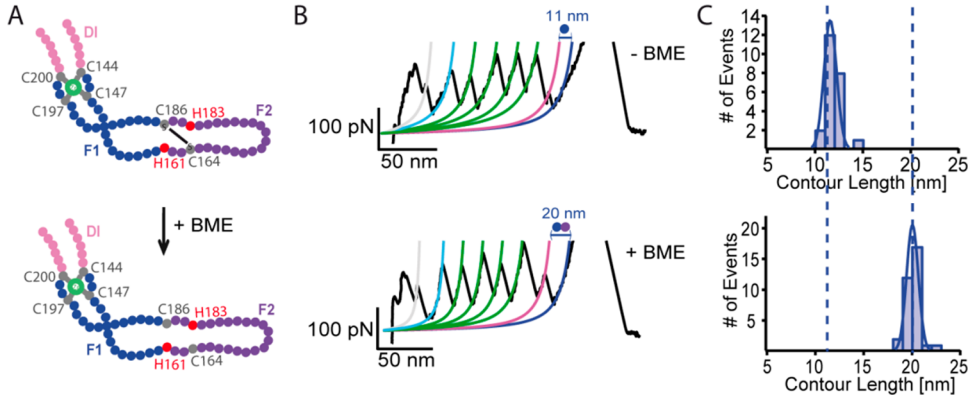

Figure 3. Nanomechanics of the zinc finger is finely regulated by the interplay between zinc binding and disulfide bond formation. (A) Schematic representation of the residues forming the second zinc finger motif in the $DnaJ_{\Delta 107(C161/183H)}$ mutant. The presence of a disulfide bond between cysteines placed in opposing chelating motifs in alternate positions is confirmed by the increase in contour length after incubation with 10 mM BME.

Zn^{2+} binding. In this case, the I27 protein was used as a molecular marker (Figure 2, yellow WLC fits). Stretching this Apo- mutant (Figure 2A, middle) resulted in unfolding trajectories lacking the mechanical signature of the two zinc fingers. In these trajectories (Figure 2B, middle), unfolding of Domain I (pink fit) elicits a longer protein extension ($\Delta L_c \sim 48$ nm, Figure 2C, middle) that includes the stretching of the amino acids that were previously hidden behind Finger 1 and Finger 2 ($\Delta L_c \sim 48$ nm = 28 nm +11 nm + 9 nm, Table S1 and Table S2). Surprisingly, this pattern was only observed in 40% of the trajectories. In the remaining 60% of the recordings (Figure 2B, bottom) an individual event at ∼90 pN (Table S3) occurred (blue fit) after the unfolding of Domain I (pink fit), which in this case was accompanied by a larger increment in contour length ($\Delta L_c \sim 33$ nm, Figure 2C, bottom) than in the wild-type case (Figure 2C, upper), but shorter than in the previous apo- form (Figure 2C, middle). This is compatible with a scenario in which a hybrid finger is formed, whereby the remaining four cysteines, two from each finger, create a new non-native zinc finger motif that coordinates a single Zn^{2+} ion (Figure 2A, bottom).

$ZnCys_4$ fingers have been described to be the most common form of fingers with predominant structural roles. However, other forms including one or two histidine ligands, leading to $ZnCys_3His$ or $ZnCys_2His_2$, are also found in structural zinc fingers,[5] and are prevalent in zinc fingers with a catalytic function.[6] In the particular case of DnaJ, several biochemical studies have suggested the capability of zinc binding in a variety of mutant proteins harboring ligands different from cysteine.[32] However, due to the ensemble averaging nature of classical biochemical techniques, it remained ambiguous to determine whether zinc was indisputably bound in a particular position within the double zinc finger structure of DnaJ. Motivated by these studies, we systematically mutated the second finger while leaving the first finger intact as a benchmark. To this end, we introduced an increasing number of histidines—ranging from 1 to 4—to rationally change the chemical environment of the putative Zn^{2+} binding site (Figure SI4).

Introducing 1 histidine through the $DnaJ_{\Delta 107(C161H)}$ mutated protein form gave rise to unfolding trajectories that consistently lacked the mechanical signature of the second finger as fingerprinted by an increase in contour length of $\Delta L_c \sim 20$ nm. Replacing two of the cysteines by histidines showed three different scenarios; if both replaced cysteines were part of the same −CXXC− chelating motif, for example, in the $DnaJ_{\Delta 107(C161/164H)}$ case, a similar trend was observed where

DOI: 10.1021/acs.jpclett.5b01371
J. Phys. Chem. Lett. 2015, 6, 3335−3340

no zinc binding was measured. By contrast, when the two histidines are introduced in opposed chelating motifs in alternate positions as in the case of $DnaJ_{\Delta 107(C161/183H)}$ (Figure 3A), disrupting the first zinc motif (Figure 3B, blue fit) extends the protein by only $\Delta L_c \sim 11$ nm (Figure 3C). This is compatible with the presence of a putative disulfide bond as confirmed by the larger extension $\Delta L_c \sim 20$ nm measured when the protein was stretched in the presence of 10 mM β-mercaptoethanol (BME). Crucially, neither BME nor DTT were able to reduce the holo wt-form of the DnaJ protein. A similar outcome was measured when the cysteines are placed facing each other within both opposing chelating motifs, as is the case of $DnaJ_{\Delta 107(C164/183H)}$. However, the presence of the disulfide bond was only observed in 71% of the cases, as hallmarked by the bimodal histogram shown in Figure SI4(iv). Finally, a conformation whereby all four cysteines were replaced by histidines, $DnaJ_{\Delta 107(C161/164/183/186H)}$ displayed the expected trend with the absence of zinc binding (Figure SI4(v)).

Refined thermodynamic experiments concluded that binding of Zn(II) to their canonical Cys_4, Cys_3His, or Cys_2His_2 sites is entropy driven and modulated by proton release.[33] Crucially, at physiological pH, the three different sites are equivalent, with an associated binding constant of 2.0×10^{12} M^{-1} that provides 16.8 kcal mol^{-1} as a driving force for protein folding and stabilization.[34] By contrast, our experiments show the non-equivalency of the different centers in DnaJ, demonstrating that the presence of all four cysteines is a strong requisite for proper Zn-mediated folding. This can be partially explained by the most favorable (by ~2 kcal mol^{-1}) binding of zinc to cysteine when compared to histidine.[34] Interestingly, even when the four cysteines do not belong to the same finger (i.e., they are physically apart in the native tertiary structure) the polypeptide can elastically deform to create a non-native hybrid zinc finger conformation. In this case, the entropic cost of loop closing[35] is overcome by the enthalpic contributions associated with zinc binding. Similarly, in the cases where two opposing cysteines are present within an individual finger, it is the disulfide bond formation that counteracts the loss of conformational entropy associated with loop closure. It is tempting to speculate that the formation of the disulfide bond in the apo- form might work as a protective mechanism that helps the structural integrity of the chaperone, which has to conduct its function under stress conditions despite the reducing conditions of its natural cytosolic environment.

The intrinsic biological function of a molecular chaperone such as this paradigmatic Type I Hsp40 involves binding to unfolded substrates to prevent their irreversible aggregation. Both Domain I, which contains a hydrophobic pocket that accommodates short peptides and regions of unfolded substrates,[36] and the Zn-Binding domain have been postulated to be involved in the binding of the unfolded proteins.[37] In particular, the small peptide APPY, exhibiting the hydrophobic sequence CALLQSRLLLSAPRRAAATARY (Figure 4A), has been shown to bind to DnaJ with high affinity, and also to Hsp70 chaperones.[27,38] Ligand (protein) binding often triggers a conformational change in the protein substrate. Such slight structural rearrangement often induces a change in the mechanical properties of the bound substrate with respect to the apo- form.[15,17,39] Stretching the $DnaJ_{\Delta 107}$ polyprotein previously incubated with a saturating concentration of APPY (150 μM) results in unfolding trajectories that globally display the same unfolding trend than that previously observed in the

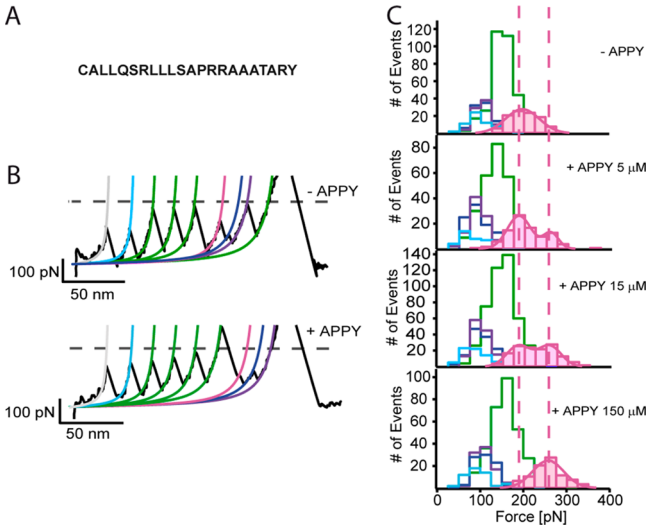

Figure 4. Binding of APPY to DnaJ significantly increases the mechanical stability of its Domain I. (A) Amino acidic sequence of the hydrophobic APPY peptide. (B) Force extension trajectories corresponding to the unfolding of $DnaJ_{\Delta 107}$ in the absence (top) or presence (bottom) of 150 μM APPY (saturating conditions). (C) Histograms corresponding to the forces associated with the different unfolding events observed for $DnaJ_{\Delta 107}$ in the absence or in the presence of APPY at different concentrations. The bound-form is fingerprinted by a ~ 50 pN increase in the unfolding force of the Domain I.

absence of peptide binding (Figure 4B). Remarkably, while APPY binding does not significantly change the unfolding forces of Domain III and the zinc fingers, it has a massive effect on the mechanical unfolding of Domain I, which is increased by as much as ~50 pN (Figure 4C). Using intermediate nonsaturating concentrations of APPY, ranging from 5 μM to 15 μM, provides a bimodal distribution in the force required to unfold Domain I, whereby the relative weight of the peak corresponding to the unbound and bound species is directly modulated by the concentration of APPY. Our observations demonstrating a localized change in mechanical stability in only one of the domains indicate that the change in the unfolding force serves as an internal, specific molecular reporter that fingerprints the binding position, of particular importance in large, multidomain proteins.

Altogether, our single molecule results provide a new piece to the puzzle of understanding the unfolding pathways of structurally complex, multidomain proteins. The interesting topology of DnaJ, harboring two functionally important zinc finger domains, is used as a platform to study the fine-tuned molecular mechanisms controlling the largely unstudied mechanochemistry of a natural zinc-containing metalloprotein.

EXPERIMENTAL METHODS

The genes codifying $DnaJ_{\Delta 107}$ and its mutants were amplified by PCR using the appropriate primers containing the restriction sites for BamHI, BglII and KpnI. All polyproteins were cloned into the pQE80L (Qiagen) expression vector and transformed into the BLR (DE3) *Escherichia coli* expression strain.

Single molecule experiments were conducted at room temperature using both a homemade setup described elsewhere[40] and a commercial Luigs and Neumann force spectrometer.[41] Each protein sample was prepared by depositing 1−5 μL of protein (at a concentration of 0.5−1.5

DOI: 10.1021/acs.jpclett.5b01371
J. Phys. Chem. Lett. 2015, 6, 3335−3340

mg/mL) onto a freshly evaporated gold cover slide. All the experiments were carried out using PBS buffer at pH 7.4. Each cantilever (Si_3N_4 Bruker MLCT-AUHW) was individually calibrated using the equipartition theorem, yielding a typical spring constant of ~15 pN/nm. The pulling speed was set at 400 nm s^{-1}. Information about the data supporting this research and conditions of access can be found by emailing research.data@kcl.ac.uk.

■ ASSOCIATED CONTENT

Supporting Information

Information on force−extension and force−clamp characterization of DnaJ, together with the nanomechanical characterization of the zinc finger for different mutants. The Supporting Information is available free of charge on the ACS Publications website at DOI: 10.1021/acs.jpclett.5b01371.

(PDF)

■ AUTHOR INFORMATION

Corresponding Author

*E-mail: sergi.garcia-manyes@kcl.ac.uk.

Notes

The authors declare no competing financial interest.

■ ACKNOWLEDGMENTS

The authors thank Josep Relat-Goberna for help in data analysis and members of the Garcia-Manyes lab for critical reading of the manuscript. We thank Arturo Muga (Bilbao, Spain) for kindly sharing the DnaJ gene. This work was supported by the Marie Curie IEF Program (329308) (to J.P.-C.), by the Marie Curie CIG Program (293462), by the BBSRC Grant BB/J00992X/1, by the EPSRC Fellowship K00641X/1 and by the Royal Society Research Grant RG120038 (all to S.G.-M).

■ REFERENCES

(1) Thomson, A. J.; Gray, H. B. Bio-Inorganic Chemistry. *Curr. Opin. Chem. Biol.* **1998**, *2*, 155−158.

(2) Sousa, S. F.; Lopes, A. B.; Fernandes, P. A.; Ramos, M. J. The Zinc Proteome: a Tale of Stability and Functionality. *Dalton Trans* **2009**, *38*, 7946−7956.

(3) Andreini, C.; Banci, L.; Bertini, I.; Rosato, A. Zinc Through the Three Domains of Life. *J. Proteome Research* **2006**, *5*, 3173−3178.

(4) Krishna, S. S.; Majumdar, I.; Grishin, N. V. Structural Classification of Zinc Fingers: Survey and Summary. *Nucleic Acids Res.* **2003**, *31*, 532−550.

(5) Laity, J. H.; Lee, B. M.; Wright, P. E. Zinc Finger Proteins: New Insights into Structural and Functional Diversity. *Curr. Opin. Struct. Biol.* **2001**, *11*, 39−46.

(6) Maret, W.; Li, Y. Coordination Dynamics of Zinc in Proteins. *Chem. Rev.* **2009**, *109*, 4682−4707.

(7) Cox, E. H.; McLendon, G. L. Zinc-Dependent Protein Folding. *Curr. Opin. Chem. Biol.* **2000**, *4*, 162−165.

(8) Beyer, M. K.; Clausen-Schaumann, H. Mechanochemistry: The Mechanical Activation of Covalent Bonds. *Chem. Rev.* **2005**, *105*, 2921−2948.

(9) Oberhauser, A. F.; Carrion-Vazquez, M. Mechanical Biochemistry of Proteins: One Molecule at a Time. *J. Biol. Chem.* **2008**, *283*, 6617−6621.

(10) Grandbois, M.; Beyer, M.; Rief, M.; Clausen-Schaumann, H.; Gaub, H. E. How Strong is a Covalent Bond? *Science* **1999**, *283*, 1727−1730.

(11) Garcia-Manyes, S.; Liang, J.; Szoszkiewicz, R.; Kuo, T. L.; Fernandez, J. M. Force-Activated Reactivity Switch in a Bimolecular Chemical Reaction. *Nat. Chem.* **2009**, *1*, 236−242.

(12) Zheng, P.; Li, H. Highly Covalent Ferric-Thiolate Bonds Exhibit Surprisingly Low Mechanical Stability. *J. Am. Chem. Soc.* **2011**, *133*, 6791−6798.

(13) Zheng, P.; Takayama, S. I. J.; Mauk, A. G.; Li, H. B. Hydrogen Bond Strength Modulates the Mechanical Strength of Ferric-Thiolate Bonds in Rubredoxin. *J. Am. Chem. Soc.* **2012**, *134*, 4124−4131.

(14) Zheng, P.; Takayama, S. J.; Mauk, A. G.; Li, H. B. Single Molecule Force Spectroscopy Reveals That Iron Is Released from the Active Site of Rubredoxin by a Stochastic Mechanism. *J. Am. Chem. Soc.* **2013**, *135*, 7992−8000.

(15) Ainavarapu, S. R.; Li, L.; Badilla, C. L.; Fernandez, J. M. Ligand Binding Modulates the Mechanical Stability of Dihydrofolate Reductase. *Biophys. J.* **2005**, *89*, 3337−3344.

(16) Cao, Y.; Yoo, T.; Li, H. Single Molecule Force Spectroscopy Reveals Engineered Metal Chelation is a General Approach to Enhance Mechanical Stability of Proteins. *Proc. Natl. Acad. Sci. U. S. A.* **2008**, *105*, 11152−11157.

(17) Hu, X.; Li, H. Force Spectroscopy Studies on Protein-Ligand Interactions: a Single Protein Mechanics Perspective. *FEBS Lett.* **2014**, *588*, 3613−3620.

(18) Martinez-Yamout, M.; Legge, G. B.; Zhang, O. W.; Wright, P. E.; Dyson, H. J. Solution Structure of the Cysteine-Rich Domain of the Escherichia coli Chaperone Protein DnaJ. *J. Mol. Biol.* **2000**, *300*, 805−818.

(19) Cheetham, M. E.; Caplan, A. J. Structure, Function and Evolution of DnaJ: Conservation and Adaptation of Chaperone Function. *Cell Stress Chaperones* **1998**, *3*, 28−36.

(20) Szabo, A.; Langer, T.; Schroder, H.; Flanagan, J.; Bukau, B.; Hartl, F. U. The ATP Hydrolysis-Dependent Reaction Cycle of the Escherichia coli Hsp70 system DnaK, DnaJ, and GrpE. *Proc. Natl. Acad. Sci. U. S. A.* **1994**, *91*, 10345−10349.

(21) Zheng, P.; Li, H. Direct Measurements of the Mechanical Stability of Zinc-Thiolate Bonds in Rubredoxin by Single-Molecule Atomic Force Microscopy. *Biophys. J.* **2011**, *101*, 1467−1473.

(22) Peng, Q.; Li, H. B. Domain Insertion Effectively Regulates the Mechanical Unfolding Hierarchy of Elastomeric Proteins: Toward Engineering Multifunctional Elastomeric Proteins. *J. Am. Chem. Soc.* **2009**, *131*, 14050−14056.

(23) Li, H. B.; Fernandez, J. M. Mechanical Design of the First Proximal Ig Domain of Human Cardiac Titin Revealed by Single Molecule Force Spectroscopy. *J. Mol. Biol.* **2003**, *334*, 75−86.

(24) Brockwell, D. J.; Beddard, G. S.; Paci, E.; West, D. K.; Olmsted, P. D.; Smith, D. A.; Radford, S. E. Mechanically Unfolding the Small, Topologically Simple Protein L. *Biophys. J.* **2005**, *89*, 506−519.

(25) Liu, R.; Garcia-Manyes, S.; Sarkar, A.; Badilla, C. L.; Fernandez, J. M. Mechanical Characterization of Protein L in the Low-Force Regime by Electromagnetic Tweezers/Evanescent Nanometry. *Biophys. J.* **2009**, *96*, 3810−3821.

(26) Banecki, B.; Liberek, K.; Wall, D.; Wawrzynow, A.; Georgopoulos, C.; Bertoli, E.; Tanfani, F.; Zylicz, M. Structure-Function Analysis of the Zinc Finger Region of the DnaJ Molecular Chaperone. *J. Biol. Chem.* **1996**, *271*, 14840−14848.

(27) Perales-Calvo, J.; Muga, A.; Moro, F. Role of DnaJ G/F-rich Domain in Conformational Recognition and Binding of Protein Substrates. *J. Biol. Chem.* **2010**, *285*, 34231−34239.

(28) Picot, D.; Ohanessian, G.; Frison, G. Thermodynamic Stability Versus Kinetic Lability of ZnS4 Core. *Chem. - Asian J.* **2010**, *5*, 1445−1454.

(29) Solomon, E. I.; Gorelsky, S. I.; Dey, A. Metal-Thiolate Bonds in Bioinorganic Chemistry. *J. Comput. Chem.* **2006**, *27*, 1415−1428.

(30) Lee, Y. M.; Lim, C. Factors Controlling the Reactivity of Zinc Finger Cores. *J. Am. Chem. Soc.* **2011**, *133*, 8691−8703.

(31) Linke, K.; Wolfram, T.; Bussemer, J.; Jakob, U. The Roles of the Two Zinc Binding Sites in DnaJ. *J. Biol. Chem.* **2003**, *278*, 44457−44466.

DOI: 10.1021/acs.jpclett.5b01371
J. Phys. Chem. Lett. 2015, 6, 3335−3340

(32) Shi, Y. Y.; Tang, W.; Hao, S. F.; Wang, C. C. Contributions of Cysteine Residues in Zn2 to Zinc Fingers and Thiol-Disulfide Oxidoreductase Activities of Chaperone DnaJ. *Biochemistry* **2005**, *44*, 1683−1689.
(33) Reddi, A. R.; Gibney, B. R. Role of Protons in the Thermodynamic Contribution of a Zn(II)-Cys(4) Site Toward Metalloprotein Stability. *Biochemistry* **2007**, *46*, 3745−3758.
(34) Reddi, A. R.; Guzman, T. R.; Breece, R. M.; Tierney, D. L.; Gibney, B. R. Deducing the Energetic Cost of Protein Folding in Zinc Finger Proteins Using Designed Metallopeptides. *J. Am. Chem. Soc.* **2007**, *129*, 12815−12827.
(35) Li, H.; Wang, H. C.; Cao, Y.; Sharma, D.; Wang, M. Configurational Entropy Modulates the Mechanical Stability of Protein GB1. *J. Mol. Biol.* **2008**, *379*, 871−880.
(36) Li, J.; Qian, X.; Sha, B. The Crystal Structure of the Yeast Hsp40 Ydj1 Complexed with its Peptide Substrate. *Structure* **2003**, *11*, 1475−1483.
(37) Szabo, A.; Korszun, R.; Hartl, F. U.; Flanagan, J. A Zinc Finger-like Domain of the Molecular Chaperone DnaJ is Involved in Binding to Denatured Protein Substrates. *EMBO J.* **1996**, *15*, 408−417.
(38) Montgomery, D. L.; Morimoto, R. I.; Gierasch, L. M. Mutations in the Substrate Binding Domain of the Escherichia coli 70 kDa Molecular Chaperone, DnaK, which Alter Substrate Affinity or Interdomain Coupling. *J. Mol. Biol.* **1999**, *286*, 915−932.
(39) Bertz, M.; Rief, M. Ligand Binding Mechanics of Maltose Binding Protein. *J. Mol. Biol.* **2009**, *393*, 1097−1105.
(40) Schlierf, M.; Li, H.; Fernandez, J. M. The Unfolding Kinetics of Ubiquitin Captured with Single-Molecule Force-ClampTechniques. *Proc. Natl. Acad. Sci. U. S. A.* **2004**, *101*, 7299−7304.
(41) Popa, I.; Kosuri, P.; Alegre-Cebollada, J.; Garcia-Manyes, S.; Fernandez, J. M. Force Dependency of Biochemical Reactions Measured by Single-Molecule Force-Clamp spectroscopy. *Nat. Protoc.* **2013**, *8*, 1261−1276.

DOI: 10.1021/acs.jpclett.5b01371
J. Phys. Chem. Lett. 2015, 6, 3335−3340